Application of EMC-J methodology in failure prediction of the U-notched polymeric specimens having a ductile behavior

H.R. Majidi [a,*], S.M.J. Razavi [b], A.R. Torabi [c]

[a] *Department of Mechanical Engineering, Iran University of Science and Technology (IUST), Narmak, 16846 Tehran, Iran*

[b] *Department of Mechanical and Industrial Engineering, Norwegian University of Science and Technology (NTNU), Richard Birkelands vei 2b,7491 Trondheim, Norway*

[c] *Fracture Research Laboratory, Faculty of New Sciences and Technologies, University of Tehran, P.O. Box 14395-1561, Tehran, Iran*

Abstract

The main purpose of the present research paper is to investigate applicability of a new energy-based failure predictive model, called EMC-J criterion to predict the critical loads of U-notched polymeric samples having a ductile behavior and loaded under symmetric three-point bending. The evaluated polymeric single edge notch bending (SENB) samples containing U-notches fractured by significant plastic deformations around the notch border making it inappropriate to directly use classic linear elastic based formulations. Due to the elastic-plastic behavior of the tested polymeric material, EMC-J criterion is applied in all of failure analyses to avoid using complex and extremely time-consuming non-linear process for failure load predictions. Finally, it is shown that EMC-J criterion can provide a good consistency between the experimental and theoretical results with an average discrepancy of about 10%.

Keywords: Equivalent Material Concept (EMC); EMC-J; Ductile; PMMA

* H.R. Majidi, Email address: h_majidi@alumni.iust.ac.ir

1. Introduction

The majority of engineering structures and their components include different kinds of notches including key-hole, O-, V- and U- notches to fulfill particular obligations in designing process; some of these obligations are load transferring from one part to another, maintaining flawed structures (cracked or damaged), making connections between different parts, etc. However, despite their useful applications, it is very likely that crack initiates from the notch because of the stress concentration located at the notch area. Obviously fracture of the component due to the propagation of the crack would then seem to be inevitable. So it is crucial to design notched structures in a specific way so that the initiation of crack from the notch border is prohibited or at least postponed [1-4]. In order to accomplish this goal, it is vitally required to predict the crack initiation with high accuracy by utilizing proper fracture criteria.

As far as the field of solid mechanics is concerned, there are three main categories of engineering materials naming ductile, quasi-brittle and brittle materials. The main difference between the most of ductile materials and the other two categories is that the strain process leading to failure happens over time and therefore the fracture occurrence is rather stable and progressive, unlike the brittle and quasi-brittle materials that fracture happens suddenly and quickly due to the low strain endurance compared to ductile materials. Researchers have spent most of their effort on brittle fracture investigation of notched components, thus ductile failure have not been the center of attention and there is a rather moderate archive of it. For this matter, there are two main reasons to discuss; firstly the failure analyses of brittle members are simple since the linear-elastic material behavior assumption is considered while analyzing. Secondly there is a probable serious damage to the structures due to the disastrous essence of brittle fracture occurrence. It is of great deal to perform failure analysis of ductile members with notches since there is a vast amount of new applications for ductile materials including aluminum alloys used in aerial vehicles; even though the analysis process of these materials which demonstrate

elastic- plastic behavior (especially the ductile metallic ones) is considerably more complicated than the analysis of brittle members with notches. In recent years, fewer researches conducted on ductile failure of notched components while undergoing different loading conditions [5-16].

Maybe, the first work in this way has been conducted by Susmel and Taylor by testing some U- and V-notched metallic specimens subjected to mode I loading. In order to achieve suitable theoretical predictions in estimating the failure load of notched components, they have utilized the Theory of Critical Distances (TCD) which is usually utilized to predict the fracture behavior of brittle materials. Although the notched components tested in [5] experienced large-scale yielding (LSY) regime, however good consistency have been observed between the experimental and theoretical prediction results. Moreover, similar researches have been published by Cicero and co-researchers [6-9], in which the load bearing capacities (LBCs) have been studied for some notched ductile samples by means of TCD methodology. Here, an important comment may be raised that *how the TCD methodology can predict well the failure load values of notched ductile components, when they have experienced a considerable yielding regime*.

To achieve a proper justification for such analyses reported in Refs. [5-9], Torabi has proposed a new theory in the field of notch fracture mechanics (NFM) entitled Equivalent Material Concept (EMC) which has been applicable in the failure prediction of ductile material exhibiting elastic-plastic behavior. According to EMC, the failure behavior of ductile materials can be equated by virtual brittle material exhibiting perfectly linear-elastic behavior. Hence, it is expected that various brittle fracture criteria like averaged strain energy density (ASED), mean stress (MS), maximum tangential stress (MTS), etc., can be coupled with the theory of EMC, providing some new EMC-based failure predictive models. For instance, it can be referred to two applicable researches [10, 11], in which the LBCs of some notched ductile steel plates and bolts have been predicted by applying the theory of EMC. Additionally, a few researches dealing with failure assessment in ductile components containing

U-notches have been recently published by Torabi and co-workers [12-16]. They have successfully published seven researches in this topic; four of them analyzed pure mode I loading, and the other works studied in-plane mixed mode I/II loading. It can be found in [12-14] that EMC has been coupled with the ASED criterion. Also, in Refs. [15, 16], the theory of EMC has been linked to the maximum tangential stress (MTS) and mean stress (MS) criteria, providing the two ductile failure predictive models, called EMC-MTS and EMC-MS. In all of these researches, an acceptable agreement can be found between the experimental data and theoretical predictions, which can be realized as a strong point of the theory of EMC.

Cicero and co-researchers [7] have tested PMMA single edge notch bending specimens (SENB) weakened by U-notches and loaded under symmetric three-point bending, experienced considerable plastic deformations around their notch border. More recently, Cicero et al. [17] have successfully combined the theory of EMC with the theory of critical distances (TCD), providing a novel failure predictive model, known as EMC-TCD methodology, to predict the fracture loads of SENB PMMA samples which have been reported previously in Ref. [7].

In two new separate researches, Majidi et al. [18, 19] have successfully linked EMC to J-integral criterion, creating a new EMC energy-based failure predictive model, known as EMC-J criterion, for analyzing ductile behavior of ductile components weakened by U-notches. In Ref. [18], they have utilized EMC-J methodology to estimate the experimental failure load results of rectangular samples containing U-notches and made of two types of Aluminum alloys (i.e. Al 7075-T6 and Al 6061-T6) which have been previously experimented under pure tensile mode I loading in [15]. Additionally, Majidi et al. [19] have estimated the experimentally obtained failure loads of U-notched rectangular plates made of Aluminum alloy 6061-T6 and subjected to mixed mode I/II loading condition by using EMC-J methodology. Finally, it was revealed that the ductile failure behavior of U-notched aluminum

samples tested under pure mode I and mixed mode I/II loading conditions has been successfully predicted, when the EMC-J criterion to be utilized.

As aforementioned, the theory of EMC has shown in recent researches that it has high capability to be coupled with different famous brittle fracture criteria, such as ASED, MTS, MS, TCD and J-integral criteria, forming some new failure models based on the theory of EMC for failure prediction of various notched members having a ductile behavior. Hence, in the present research, it is attempted to investigate the capability of EMC-J failure model, in prediction of ductile behavior in U-notched PMMA samples under symmetric three point bending loading. In this way, seven sets of experiments on ductile failure of SENB PMMA samples are first gathered form the literature [7]. Then, EMC-J criterion is utilized in order to estimate the experimental critical loads of the PMMA samples. Note that no research paper could be found during literature survey in the topic of failure prediction of notched polymeric specimens like PMMA failed by considerable yielding regime, by applying of EMC-J predictive model. This is the novelty of this research paper.

2. Experimental results on SENB samples

In 2012, Cicero et al. [7] worked on experimental research in which seven sets experiments have been conducted for providing pure tensile mode I fracture in U-notched specimens. The material tested in [7] was a type of polymethyl-methacrylate (PMMA) with the main material parameters listed in Table 1. Note that the researcher of Ref. [7] not reported the Poisson's ratio of the PMMA tested in [7]. However, since the value of υ has been reported in many researches approximately equal to 0.4 (see for instances [20-22]), the authors considered the same value in the analyses [20-22]. The engineering tensile stress-strain curves of the PMMA tested in [7], revealed that it has clear non-linear behaviour in its failure mechanism (see Fig. 1).

Table 1 Material properties of the PMMA tested in Ref. [7].

Material property	Value
Elastic modulus (GPa)	3.4
Poisson's ratio	0.4
Ultimate tensile strength (MPa)	74.5
Fracture toughness (MPa.m$^{0.5}$)	2.04

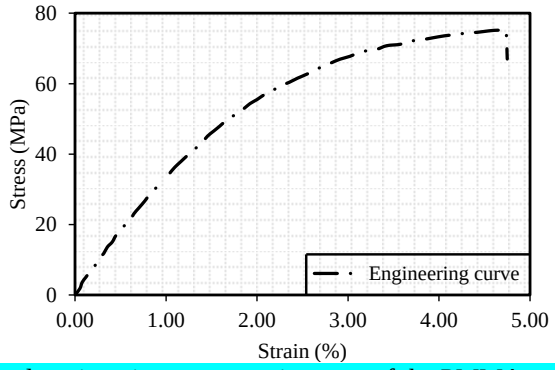

Fig. 1. Typical engineering stress-strain curve of the PMMA tested in [17].

Single edge notch bending specimens containing U-notches with the thickness of 5 mm were tested under pure mode I loading condition. Details of the experimental programs were presented by Cicero et al. in Ref. [7]. Fig. 2 illustrates the three-dimensional view of SENB sample. Also, the parameters ρ, a, t, L_1, L_2, W, and P have been introduced in Fig. 2. Seven size of notch tip radius have been considered (i.e. from 0.25 to 2.5 mm) [7]. The length of notch has also been equal to 5 mm. The applied loading rate equal to 10 mm/min was applied in all of experiments. Each experiment has been conducted in five times, preparing an excellent checking the repeatability of the experimental results. Some sources of error were found in some experimental results. Therefore, a total number of 29 experimental results for U-notches have been reported in [7]. The experimental critical loads of the tested SENB PMMA specimens are presented in Table 2. As is shown in Table 2, each specimen is characterized by a specific code as, ρ-n. For instance, the specific code 0.5-2 relates to a second tested SENB sample with ρ = 0.5 mm.

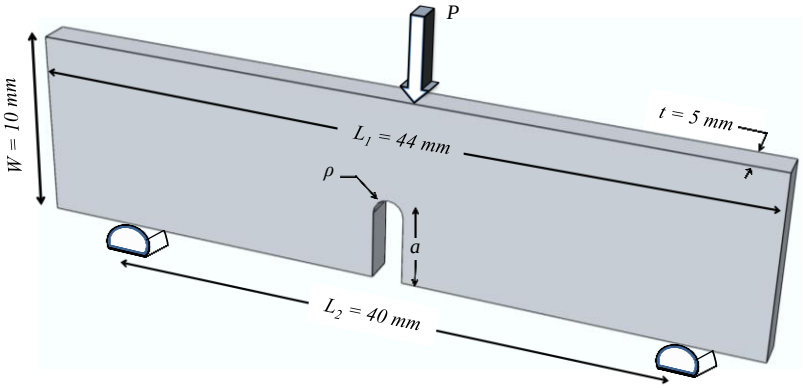

Fig. 2. The SENB test sample loaded under symmetric three point bending [7].

Table 2 Summary of the experimental results related to tested SENB samples [7].

Specimen index	Experimental failure load $P_{exp.}$ (N)
0.25-1	124.9
0.25-2	119.9
0.25-3	104.0
0.25-4	107.1
Average	113.9
0.32-1	117.4
0.32-2	112.6
0.32-3	102.5
0.32-4	108.7
Average	110.3
0.5-1	90.0
0.5-2	85.2
0.5-3	170.3
0.5-4	162.6
Average	127.0
1.0-1	212.8
1.0-2	213.6
1.0-3	204.8
1.0-4	202.8
1.0-5	202.6
Average	207.3
1.5-1	215.5
1.5-2	165.9
1.5-3	219.0
1.5-4	197.9
Average	199.6
2.0-1	258.5
2.0-2	261.1
2.0-3	237.8
Average	252.5
2.5-1	253.8
2.5-2	259.9
2.5-3	250.4
2.5-4	251.3
2.5-5	243.2
Average	251.7

Cicero et al. [7] reported that significant plastic deformations, particularly for higher notch radii, were occurred for the tested notched PMMA specimens. In fact, the plastic region starts from the notch border and consequently, a crack initiates from a location at the notch border and propagates slowly until to happening a fracture moment. Hence, it has not been expected that the failure predictive models followed the rules of linear elastic NFM (LENFM), can be used to predict the experimental critical loads of the PMMA SENB specimens. For solving this problem, the authors suggest that, the theory of EMC can be useful to provide a new ductile failure predictive model. Hence, in the next section, EMC is briefly expressed and in the forthcoming, the EMC-J criterion has been elaborated, providing a prediction of fracture loads of the SENB PMMA samples loaded under symmetric pure mode I loading condition.

3. A brief description of the Equivalent Material Concept

In order to replace the extremely time-consuming and also rather intricate elastic-plastic failure analysis of notched members by an equivalent linear-elastic one, Torabi [10] has presented the theory of Equivalent Material Concept. Initially, two assumptions have been made to formulate the elastic-plastic behavior of a real ductile material to the linear-elastic behavior of a virtual brittle material till the fracture moment [10];

1) The equivalent brittle materials and the real ductile have the same values of Young's modulus and fracture toughness, while they have different values of the tensile strength.

2) Equal absorption of the SED was assumed for both materials when crack is initiated under tensile loading.

The tensile strength of the equivalent material has been calculated by combining the power-law equation which considers plastic behavior of the real ductile material using the stress-strain relationship

and the SED formulation for brittle materials at the point when the crack growth commences. Thus, the tensile strength of the equivalent material (σ_f^*) can be evaluated by the following formulation [12-14]:

$$\sigma_f^* = \sqrt{\sigma_y^2 + \frac{2EK}{n+1}[{\varepsilon_{u,true}}^{n+1} - (0.002)^{n+1}]} \quad (1)$$

In which the parameters σ_y and σ_f^* denote the yield strength of the ductile material and the tensile strength of the equivalent material, respectively. Also, the strain-hardening exponent, the true plastic strain at the ultimate point, the elastic modulus, the strain-hardening coefficient have been introduced by the parameters n, $\varepsilon_{u,true}$, E, K, respectively. Also, the parameter $\varepsilon_{u,true}$ can be evaluated by using Eq. (2) as follows:

$$\varepsilon_{u,true} = Ln(1 + \varepsilon_u) \quad (2)$$

The value of σ_f^* can be obtained for the PMMA tested in [7] by suitable substitution of the data, from Table 1 into Eq. (1). This value is approximately equal to 129.4 MPa. After the estimations, it is possible to predict the critical load of the notched part on the equivalent material by using the calculated values of σ_f^* = 129.4 MPa and K_c = 2.04 MPa.m$^{0.5}$ in different brittle fracture models, like J-integral criterion, which are applicable for the notch fracture mechanics based on linear-elastic assumptions. It is worth mentioning that the prediction is expected to be similar to the notched part of the real ductile material.

4. EMC-J criterion for U-notches

The J-integral was proposed with the purpose to describe the local stress concentration fields and also the crack propagation around the cracks and notches in cracked and notched members. In fact, the basic work of the J-integral is evaluating the release rate of strain energy for any engineering material. Rice [23] was the first one who proposed J-integral formulation for various structures containing cracks and

notches. In the next decades, many researches dealing with J-integral concept were published in the scientific literature for different cracked and notched components under various loading conditions [24-27]. Recently, a new expression of J-integral, called EMC-J criterion has been proposed to estimate the failure loads of U-notched ductile experimental samples for the conditions of mode I and mixed mode I/II loadings [18, 19]. In the current research, the EMC-J criterion is used for failure load prediction of polymeric specimens containing U-notch and experiencing large plasticity before the final fracture.

4.1. A general expression of J-integral

J-integral equation can generally be evaluated by the two following integrals [23]:

$$J_1 = \oint_{\varphi} \left(W dy - T_i \frac{\partial u_i}{\partial x} ds \right) \tag{3}$$

$$J_2 = \oint_{\varphi} \left(W dx - T_i \frac{\partial u_i}{\partial y} ds \right) \tag{4}$$

in which the parameter SED has been denoted by W in Eq. (1). Also, the components u_i, T_i exist in the above equations are the displacement and traction vectors, respectively. Note that the x axis should be coincided with the notch bisector line (see Fig. 3). It is notable that for the mixed mode I/II loading condition, both values of J-integrals (i.e. J_1 and J_2) play role in the theoretical predictions. So, the total value of J-integral can be evaluated by utilizing Eq. (5) as follows:

$$J_{eq} = \sqrt{{J_1}^2 + {J_2}^2} \tag{5}$$

4.2. How to evaluate the value of J-integral for mode I loading condition?

In some recent researches in which ASED criterion has been utilized [28, 29], have been reported that the shape of control volume for U-notches is a crescent shape. Fig. 3 shows that the specified control volume is located at the notch tip for mode I loading conditions. It is seen in Fig. 3 that the parameter R_c is a critical radius and relates only to the material properties. Yosibash et al. [30] have suggested the

following formulation to compute the value of critical radius of the control volume for the plane strain conditions.

$$R_c = \frac{(1+\upsilon)(5-8\upsilon)}{4\pi}\left(\frac{K_{Ic}}{\sigma_u}\right)^2 \tag{6}$$

in which three material components, including the ultimate tensile strength (σ_u), the Poisson's ratio (υ), and the plane-strain fracture toughness (K_{Ic}) have played roles in the value of critical radius for brittle materials.

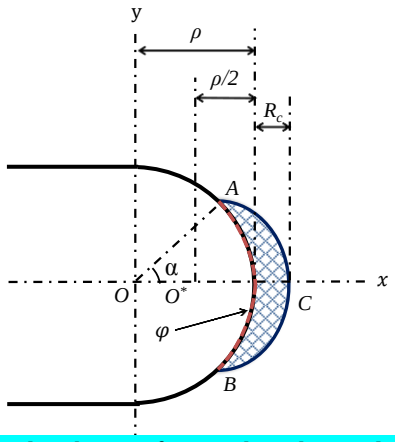

Fig. 3. Control volume located at the tip of U-notch in the condition of pure mode I loading.

As can be seen in Fig. 3, a crescent-shaped control volume is resulted between the two arcs with different curvatures. The outer radius of the crescent control volume is equal to $R_c + \rho/2$, while the inner arc is located around the notch border. Note that the centers of these two curves have been located according to the coordinate systems shown in Fig. 3.

Furthermore, note that x axis should be coincided with the notch bisector line (as is shown in Fig. 3) resulting a zero value for J_2. The inner arc of AB should be considered as a specified integration path. Since the traction-free conditions exist on the inner arc of crescent shaped of the control volume, the second term of J-integral equation vanishes. Therefore, the following expression can be utilized to evaluate the J-integral parameter for U-notches loaded under pure mode I:

$$J = \oint_{\varphi} W dy = W_1(y_2 - y_1) + W_2(y_3 - y_2) + W_3(y_4 - y_3) + \cdots + W_{n-1}(y_n - y_{n-1}) \quad (7)$$

To provide a simple form of Eq. 7, the polar coordinate system located at point O, should be considered. Thus, Eq. (7) can be written as:

$$J = \int_{-\alpha}^{+\alpha} W(\theta)\rho cos(\theta)\, d\theta \quad (8)$$

Also in order to provide a simple expression of Eq. (8), it is firstly suggested that the SED distribution along the specified integration path (i.e. the inner arc of the control volume) should be evaluated by using the following formulation [24, 25]:

$$W(\theta) = W_{max} cos^{\delta}(\theta) \quad (9)$$

In fact, the exponent δ can be obtained by fitting the SED distributions around the notch border to its cosine distribution form. Also, It is obvious that the maximum SED (i.e. W_{max}) exists at the notch tip and it can be reported directly by means of finite element (FE) analysis. Thus, Eq. (9) can be simply written as [31]:

$$J = 2\rho W_{max} \int_0^{\alpha} cos^{\delta+1}(\theta)\, d\theta = 2\rho W_{max} \Delta \quad (10)$$

in which the exponent Δ can be evaluated numerically by the following integral:

$$\Delta = \int_0^{\alpha} cos^{\delta+1}(\theta)\, d\theta \quad (11)$$

Now, the calculation process of the J-integral parameter has been finished.

4.3. How to evaluate the theoretical predictions based on EMC-J criterion?

As aforementioned, the J-integral parameter has played a main role in the J-integral criterion. Barati and Berto [26] have claimed that according to J-integral criterion, failure occurs when the value of J-integral over a specified path around the notch border attains to the critical value of J-integral (i.e. J_{cr}).

They have proposed the following formulation for evaluating the J_{cr} of U-notches loaded under pure mode I [26]:

$$J_{cr} = \frac{2\sigma_u^2 \rho \Delta (1-\upsilon^2)}{\pi H E} \tag{12}$$

Lazzarin and Berto [28] have shown that the parameter H in Eq. 12 relates all stresses and strains component on the control volume, hence, this value depends on the normalized radius R_c/ρ and the Poisson's ratio ν. Table 3 lists the values of H relating to pure mode I loading in U-notched specimens.

Table 3 Numerical results of the parameter H for U-notched samples under plane strain conditions [28].

R_c/ρ (mm)	H		
	υ = 0.3	υ = 0.35	υ = 0.4
0.001	0.5777	0.5570	0.5332
0.002	0.5761	0.5555	0.5316
0.003	0.5746	0.5539	0.5300
0.004	0.5730	0.5524	0.5285
0.005	0.5715	0.5508	0.5270
0.006	0.5699	0.5493	0.5255
0.008	0.5668	0.5462	0.5225
0.01	0.5638	0.5432	0.5194
0.02	0.5490	0.5285	0.5049
0.03	0.5349	0.5145	0.4910
0.04	0.5214	0.5011	0.4778
0.05	0.5086	0.4884	0.4652
0.06	0.4962	0.4761	0.4531
0.07	0.4844	0.4645	0.4416
0.08	0.4731	0.4533	0.4306
0.1	0.4518	0.4322	0.4099
0.2	0.3670	0.3488	0.3283
0.3	0.3069	0.2902	0.2713
0.4	0.2622	0.2468	0.2295
0.5	0.2276	0.2135	0.1976
0.6	0.2000	0.1817	0.1725
0.7	0.1775	0.1655	0.1522
0.8	0.1591	0.1480	0.1357

Now, the EMC-J-integral criterion is utilized here by considering the mechanical properties resulted from the EMC expression to predict the critical loads of the SENB samples weakened by U-notches. To this aim, the tensile strength of the equivalent material (i.e. σ_f^*) should be utilized instead of σ_u in

Eqs. 7 and 14. Moreover, the critical radius R_c should be computed to evaluate the H value for each notched specimen. Thus, by considering $\sigma_u = \sigma_f^*$ (σ_f^* values are equal to 129.4 MPa for the tested PMMA) and using Eq. 7, the value of the control radius for the equivalent material (i.e. $R_{c/EMC}$) is obtained to be equal to 0.0498 mm. Moreover, by considering again $\sigma_u = \sigma_f^*$, a new material parameter, called $J_{cr/EMC}$, is provided as follows [18, 19]:

$$J_{cr/EMC} = \frac{2(\sigma_f^*)^2 \rho \Delta (1-\upsilon^2)}{\pi H E} \tag{13}$$

So, by means of Eqs. 10 and 13, one can simply evaluate the two main parameters of EMC-J criterion, namely the J-integral and critical J-integral for U-notches located in the SENB specimens virtually made of the equivalent material subjected to pure mode I loading. In this way, the distribution of SED along the specified curved path located around the notch border, which was obtained by using the FE analysis, is considered for each SENB specimen. Thus, A FE model is created for each U-notched specimen and after that, the linear elastic SED distribution along the specified contour path located at the notch border is evaluated. The FE models were meshed by CPE8R element type. Refined meshes have been considered at the notch border due to the high stress gradient. The minimum element size equal to 0.01 mm has been applied around the notch border for all of FE analyses (see Fig. 4). Fig. 5 illustrates the distributions of SED around the notch border for the tested SENB specimen with ρ = 1 mm.

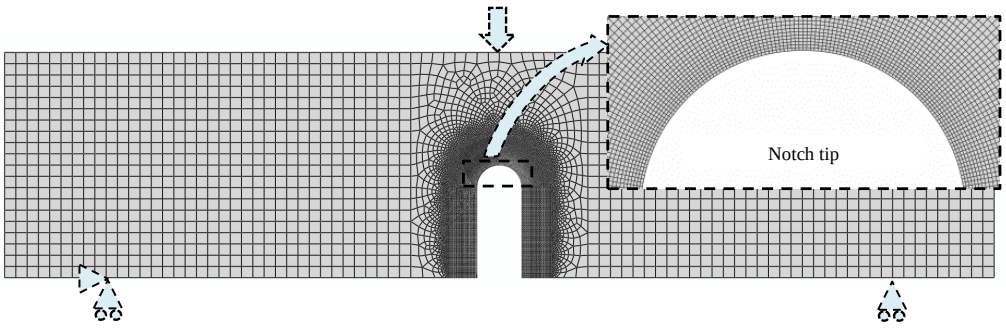

Fig. 4. Typical mesh pattern of SENB specimen in FE software.

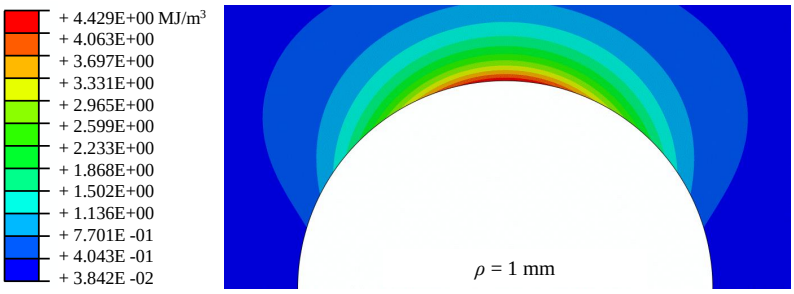

Fig. 5. Contour plot of the SED at integration points located around the notch border for the SENB sample.

Table 4 Summary of the numerical results essentially needed for evaluating the value of J-integral for SENB samples loaded under pure mode I.

ρ (mm)	$P_{av.}$ (N)	W_{max} (MPa)	arc (ACB) (mm)	J (N/mm)
0.25	113.9	4.35	0.352	1.22
0.32	110.3	3.25	0.389	1.06
0.5	127.0	2.91	0.472	1.22
1.0	207.3	4.43	0.649	2.69
1.5	199.6	3.08	0.781	2.29
2.0	252.5	4.12	0.905	3.57
2.5	251.7	3.61	1.009	3.51

Table 5 Summary of the numerical results for determining the values of J_{cr} for SENB specimens under mode I loading.

ρ (mm)	R_c/ρ	H	Δ	$J_{cr/EMC}$ (N/mm)
0.25	0.199	0.3290	0.56	1.12
0.32	0.156	0.3617	0.51	1.19
0.5	0.100	0.4099	0.42	1.35
1.0	0.050	0.4652	0.30	1.72
1.5	0.033	0.4870	0.25	2.01
2.0	0.025	0.4979	0.22	2.29
2.5	0.020	0.5049	0.19	2.53

Table 4 lists the numerical results of the two important components W_{max} and J for different notch tip radii. Note that the numerical values reported in Table 4 are obtained by applying the average experimental fracture loads, (i.e. $P_{av.}$) to the FE analyses. Table 5 presents the critical J-integral parameter together with the numerical values (i.e. the parameters H, and Δ), which have played main roles in evaluating this important parameter. All in all, it can be stated that for evaluating the critical load of a SENB PMMA sample tested under pure mode I loading condition, one should first evaluate

the parameter J-integral by considering an arbitrary load in the FE analysis and after that, the critical load is obtained when the value of J_{eq} attains $J_{cr/EMC}$.

5. Results and discussion

Cicero et al. [17] have previously predicted theoretically the experimental results investigated in [7] by applying EMC combined with the TCD criterion which is based on two methodologies, called point method and line method. Thus these criteria have been known as EMC-TCD (PM) and EMC-TCD (LM), respectively. Additionally, a new energy-based ductile failure model, known as EMC-J criterion is used here to estimate the experimental critical loads of the SENB PMMA samples tested in [14]. Hence, three separate theoretical predictions of critical load are investigated here for the SENB PMMA samples.

Table 6 presents the experimental data of critical load together with the theoretical prediction results evaluated by the two EMC-TCD combined criteria, namely the EMC-TCD (PM) and EMC-TCD (LM) criteria, and also EMC-J criterion for the SENB PMMA samples. Also, to understand better the level of efficiency in each EMC-based failure model, especially that of investigated in this research paper (i.e. EMC-J), the level of accuracy obtained from the three prediction models are studied in Table 6. As it is obvious from the data reported in Table 6, an acceptable consistency exists between the experimentally obtained critical loads and the theoretical values evaluated from EMC-J criterion and also, the other prediction values were previously re-predicted by means of the two EMC combined with TCD criteria in Ref. [17]. As can be noticed in Table 6, the average discrepancies regarding the EMC-TCD (PM) and EMC-TCD (LM) criteria are obtained to be equal to 7.6% and 13.4%, respectively, while they are obtained for the EMC-J criterion to be equal to 10.9%.

Table 6 Details of experimental critical loads with theoretical predictions for the SENB PMMA samples by means of EMC-based criteria.

ρ (mm)	$P_{av.}$ (N)	$P_{EMC\text{-}PM}$ (N) [17]	$\Delta_{EMC\text{-}PM}$ (%)	$P_{EMC\text{-}LM}$ (N) [17]	$\Delta_{EMC\text{-}LM}$ (%)	$P_{EMC\text{-}J}$ (N)	$\Delta_{EMC\text{-}J}$ (%)
0.25	113.9	111.0	2.6	128.1	12.4	109.3	4.0
0.32	110.3	119.4	8.2	135.8	23.1	116.7	5.8
0.5	127.0	139.0	9.4	153.8	21.1	133.5	5.1
1.0	207.3	183.6	11.7	195.3	6.1	165.7	20.1
1.5	199.6	219.4	9.9	229.4	14.9	186.9	6.4
2.0	252.5	250.2	0.9	259.1	2.6	202.3	19.9
2.5	251.7	277.7	10.3	285.7	13.5	213.9	15.0
Average discrepancies			**7.6 %**		**13.4 %**		**10.9%**

According to the data presented in Table 6, the EMC-TCD (PM) criterion has the best performance in the two viewpoints of accuracy and amount of calculations in predicting fracture loads of the SENB PMMA specimens, and the second rank in these viewpoints has been appertained to EMC-J criterion. Although both of the EMC-TCD (LM) and EMC-J criteria have been worked by the same amount of numerical calculations, the EMC-J criterion should be preferred because of its high accuracies with respect to the other one. Finally, for proposing a final conclusion, maybe it's better to state that EMC-TCD (PM) criterion can be of interest for designers and engineers in cases, which require low amount of numerical calculations and relatively high accuracy. Also, it is very important to note that in cases engineers require just acceptable accuracies, using each of the two EMC-TCD (LM) and EMC-J criteria can be a good decision. Trivially, each of the mentioned EMC-based failure criteria has some strong and weak points in fracture prediction of notched components, which are failed by considerable yielding regime. Hence, these failure models have been mostly utilized to be used for different experimental results of various notched specimens in order to find their advantageous and disadvantageous. Consequently, it can be stated that, if one of the EMC-based criteria succeeded in theoretical failure prediction with high performance does not delivered this message that other EMC-based failure models could not be utilized and developed. As a result, the engineers and designers should properly response to this comment that *which one of the failure models combined with the theory of EMC, could be applicable in their own works*. In fact, four important factors, namely the

engineering applications, the grade of complexity, the time of computational process, and the precision of proposed criterion should generally be considered to make a proper decision.

6. Conclusion

The present research provides a theoretical assessment for prediction of critical loads of the SENB PMMA components weakened by U-notches and loaded under symmetric three point bending. For this aim, seven sets of experiments of some U-notched specimens were gathered from the recent research reported in the literature and after that, the EMC-J criterion were utilized to estimate fracture loads of the U-notched PMMA specimens. Finally, it was shown that EMC-J criterion can be considered as an efficient ductile failure model for prediction of the fracture loads of the SENB PMMA specimens experienced significant yielding regime. Finally, using EMC-J criterion in this research proved that ductile failure prediction for the SENB PMMA components loaded under pure mode I do not essentially require complex and extremely time-consuming elastic-plastic calculations in the failure analyses of prediction process.

References

[1] M. Ayatollahi, S. Razavi, H. Chamani, A numerical study on the effect of symmetric crack flank holes on fatigue life extension of a SENT specimen, Fatigue & Fracture of Engineering Materials & Structures, 37 (2014) 1153-1164.

[2] M. Ayatollahi, S. Razavi, H. Chamani, Fatigue life extension by crack repair using stop-hole technique under pure mode-I and pure mode-II loading conditions, Procedia Engineering, 74 (2014) 18-21.

[3] M.R. Ayatollahi, S.M.J. Razavi, M.Y. Yahya, Mixed mode fatigue crack initiation and growth in a CT specimen repaired by stop hole technique, Engineering Fracture Mechanics, 145 (2015) 115-127.

[4] S. Razavi, M. Ayatollahi, C. Sommitsch, C. Moser, Retardation of fatigue crack growth in high strength steel S690 using a modified stop-hole technique, Engineering Fracture Mechanics, 169 (2017) 226-237.

[5] L. Susmel, D. Taylor, On the use of the Theory of Critical Distances to predict static failures in ductile metallic materials containing different geometrical features, Eng. Fract. Mech., 75 (2008) 4410-4421.

[6] S. Cicero, V. Madrazo, I. Carrascal, R. Cicero, Assessment of notched structural components using failure assessment diagrams and the theory of critical distances, Eng. Fract. Mech., 78 (2011) 2809-2825.

[7] S. Cicero, V. Madrazo, I. Carrascal, Analysis of notch effect in PMMA using the Theory of Critical Distances, Eng. Fract. Mech., 86 (2012) 56-72.

[8] S. Cicero, V. Madrazo, T. García, The Notch Master Curve: A proposal of Master Curve for ferritic–pearlitic steels in notched conditions, Eng. Fail. Anal., 42 (2014) 178-196.

[9] S. Cicero, T. García, V. Madrazo, Application and validation of the Notch Master Curve in medium and high strength structural steels, J. Mech. Sci. Technol., 29 (2015) 4129-4142.

[10] A.R. Torabi, Estimation of tensile load-bearing capacity of ductile metallic materials weakened by a V-notch: The equivalent material concept, Mater. Sci. Eng., A, 536 (2012) 249-255.

[11] A. Torabi, On the use of the equivalent material concept to predict tensile load-bearing capacity of ductile steel bolts containing V-shaped threads, Engineering Fracture Mechanics, 97 (2013) 136-147.

[12] A. Torabi, A. Campagnolo, F. Berto, Mixed mode I/II crack initiation from U-notches in Al 7075-T6 thin plates by large-scale yielding regime, Theor. Appl. Fract. Mech., 86 (2016) 284-291.

[13] A. Torabi, F. Berto, A. Campagnolo, J. Akbardoost, Averaged strain energy density criterion to predict ductile failure of U-notched Al 6061-T6 plates under mixed mode loading, Theor. Appl. Fract. Mech., (2017).

[14] A. Torabi, F. Berto, S. Razavi, Tensile failure prediction of U-notched plates under moderate-scale and large-scale yielding regimes, Theor. Appl. Fract. Mech., (2017).

[15] A. Torabi, R. Habibi, B.M. Hosseini, On the ability of the equivalent material concept in predicting ductile failure of U-notches under moderate-and large-scale yielding conditions, Phys. Mesomech., 18 (2015) 337-347.

[16] A. Torabi, R. Habibi, Investigation of ductile rupture in U-notched Al 6061-T6 plates under mixed mode loading, Fatigue Fract. Eng. Mater. Struct., 39 (2016) 551-565.

[17] S. Cicero, A. Torabi, V. Madrazo, P. Azizi, Prediction of fracture loads in PMMA U-notched specimens using the equivalent material concept and the theory of critical distances combined criterion, Fatigue Fract. Eng. Mater. Struct., (2017).

[18] H. Majidi, M. Golmakani, A. Torabi, On combination of the equivalent material concept and J-integral criterion for ductile failure prediction of U-notches subjected to tension, Fatigue Fract. Eng. Mater. Struct. (in press). (2018).

[19] H. Majidi, A. Torabi, M. Golmakani, J-integral expression for mixed mode I/II ductile failure prediction of U-notched Al 6061-T6 plates under large-scale yielding regime, Eng. Fract. Mech., 195 (2018) 253-266.

[20] F. Berto, P. Lazzarin, F. Gómez, M. Elices, Fracture assessment of U-notches under mixed mode loading: two procedures based on the ‘equivalent local mode I’concept, International Journal of Fracture, 148 (2007) 415.

[21] F. Gómez, M. Elices, F. Berto, P. Lazzarin, A generalised notch stress intensity factor for U-notched components loaded under mixed mode, Engineering Fracture Mechanics, 75 (2008) 4819-4833.

[22] F. Berto, M. Elices, P. Lazzarin, M. Zappalorto, Fracture behaviour of notched round bars made of PMMA subjected to torsion at room temperature, Engineering Fracture Mechanics, 90 (2012) 143-160.

[23] J.R. Rice, A path independent integral and the approximate analysis of strain concentration by notches and cracks, in, ASME, 1968.

[24] Y.G. Matvienko, J-estimation formulas for nonlinear crack problems, Int. J. Fract., 68 (1994) R15-R18.

[25] Y.G. Matvienko, E. Morozov, Calculation of the energy J-integral for bodies with notches and cracks, Int. J. Fract., 125 (2004) 249-261.

[26] E. Barati, F. Berto, A comparison between rapid expressions for evaluation of the critical J-integral in plates with U-notches under mode I loading, J. Strain Anal. Eng. Des., 46 (2011) 852-865.

[27] E. Barati, M. Azimi, Use of J-integral for prediction of critical fracture load in plates with U-notches under mixed mode loading, Theor. Appl. Fract. Mech., 82 (2016) 51-58.

[28] P. Lazzarin, F. Berto, Some expressions for the strain energy in a finite volume surrounding the root of blunt V-notches, Int. J. Fract., 135 (2005) 161-185.

[29] F. Berto, P. Lazzarin, C. Marangon, Brittle fracture of U-notched graphite plates under mixed mode loading, Mater. Des., 41 (2012) 421-432.

[30] Z. Yosibash, A. Bussiba, I. Gilad, Failure criteria for brittle elastic materials, Int. J. Fract., 125 (2004) 307-333.

[31] F. Berto, P. Lazzarin, Relationships between J-integral and the strain energy evaluated in a finite volume surrounding the tip of sharp and blunt V-notches, Int. J. Solids Struct., 44 (2007) 4621-4645.

Figure captions

Fig. 1. Typical engineering stress-strain curve of the PMMA tested in [17].

Fig. 2. The SENB test sample loaded under symmetric three point bending [7].

Fig. 3. Control volume located at the tip of U-notch in the condition of pure mode I loading.

Fig. 4. Typical mesh pattern of SENB specimen in FE software.

Fig. 5. Contour plot of the SED at integration points located around the notch border for the SENB sample.

Table captions

Table 1. Material properties of the PMMA tested in Ref. [7].

Table 2. Summary of the experimental results related to tested SENB samples [7].

Table 3. Numerical results of the parameter H for U-notched samples under plane strain conditions [28].

Table 4. Summary of the numerical results essentially needed for evaluating the value of J-integral for SENB samples loaded under pure mode I.

Table 5. Summary of the numerical results for determining the values of J_{cr} for SENB specimens under mode I loading.

Table 6. Details of experimental critical loads with theoretical predictions for the SENB PMMA samples by means of EMC-based criteria.